RESULTS FROM H1

T. GREENSHAW
Oliver Lodge Laboratory, Liverpool University,
Liverpool L69 7ZE, ENGLAND
E-mail: green@hep.ph.liv.ac.uk

Recent H1 measurements of neutral and charged current deep-inelastic scattering (DIS) e^+p cross sections are presented, as are the results of searches for physics beyond the standard model. The progress made in understanding the hadronic final state in DIS is described and some remaining problems pointed out. Event shape studies, using the power correction ansatz, are presented. The extraction of the gluon density in the proton using charm events in DIS is discussed and the cross-section for the photoproduction of open beauty is given. Recent results obtained in the study of rapidity gap events are presented.

1 Introduction

The positron proton collider HERA at DESY recently completed its most successful running period yet, providing the H1 and ZEUS experiments with a luminosity of $34\,\mathrm{pb}^{-1}$ in 1997, as much as in the previous five years put together. This, together with further analysis of the earlier data and a deepening theoretical understanding of deep-inelastic scattering and photoproduction processes has allowed significant progress to be made in the study of positron-proton collisions. Some of the areas in which that progress has been particularly marked are discussed here.

2 High Q^2 events and searches for new physics

2.1 Introduction

The new data have allowed the H1 collaboration to further study the high Q^2, high x region of the DIS kinematic plane in which an unexpectedly large number of events was found in the data taken in the years 1994 to 1996 [1,2]. The H1 collaboration observed $N_{obs} = 12$ events with $Q^2 > Q^2_{min} = 15\,000\,\mathrm{GeV}^2$ where only $N_{SM} = 4.71 \pm 0.76$ were expected from Standard Model (SM) calculations. The probability of such a measurement, assuming the SM to be correct, is $\mathcal{P}(N \geq N_{obs}) \sim 1\%$. Further, these high Q^2 events tended to be at high y and to be clustered around an electron-quark invariant mass of $M = \sqrt{xs} \sim 200\,\mathrm{GeV}$, *i.e.* at an x of about 0.4, raising the prospect that the excess events were due to leptoquark production or R-parity violating SUSY processes. The requirements $187.5 < M < 212.5\,\mathrm{GeV}$ and $y > 0.4$

Table 1: Numbers of NC events observed and expected in the SM for various Q^2_{min} values with the probabilities of the observations occuring assuming the SM to be correct.

1997 Data, H1 Preliminary						
Q^2_{min} GeV^2	2 500	5 000	10 000	15 000	20 000	25 000
N_{obs}	753	178	31	10	4	2
N_{SM}	758 ±57.9	199.7 ±17.6	32.7 ±3.8	8.77 ±1.26	2.61 ±0.43	0.94 ±0.17
$\mathcal{P}(N \geq N_{obs})$	53%	83%	59%	38%	27%	24%

1994 ...97 Data, H1 Preliminary						
Q^2_{min} GeV^2	2 500	5 000	10 000	15 000	20 000	25 000
N_{obs}	1 297	322	51	22	10	6
N_{SM}	1 276 ±98	336 ±29.6	55.0 ±6.42	14.8 ±2.13	4.39 ±0.73	1.58 ±0.29
$\mathcal{P}(N \geq N_{obs})$	42%	56%	60%	5.9%	1.8%	0.64%

Table 2: Numbers of CC events observed and expected in the SM for various Q^2_{min} values.

1994 ...97 Data, H1 Preliminary				**1994 ...96**
Q^2_{min} GeV^2	2 500	7 500	15 000	15 000
N_{obs}	100	41	9	4
N_{SM}	95.3 ±16.7	27.6 ±8.4	5.07 ±2.8	1.77 ±0.4

were satisfied by 7 events, where only 0.95 ± 0.18 were expected. The results obtained from the 1997 data are discussed in the following.

2.2 Event rates at high Q^2 and x

The number of NC DIS events with $Q^2 > 15\,000\,\mathrm{GeV}^2$ observed in 1997 was 10, which is to be compared with an expectation of 8.77 ± 1.26 events. This corresponds to a probability of about 40%. Considering all the 1994...97 data, these numbers become 22 events observed for an expectation of 14.8 ± 2.13, with probability about 6%. It is apparent that the new data have led to a decrease in the significance of the observed excess over SM expectations for $Q^2 > 15\,000\,\mathrm{GeV}^2$. Nonetheless, as can be seen from table 1, the observed number of NC events at the highest Q^2 values remains significantly larger than expected from the SM. The situation for CC events is summarised in table 2. Again, though here with lower significance, the number of events at large Q^2 is higher than expected. The clarification of this puzzle demands a significant increase in the luminosity available to the H1 and ZEUS experiments, which will become available following the HERA upgrade in the year 2000 [3].

2.3 Leptoquark searches

Given the above observations, it is important to examine carefully the possibility that leptoquarks (LQs) are being produced at HERA. The H1 collaboration has extended earlier searches for LQs [4], as is discussed in detail elsewhere [5]. If LQs decay primarily to electron-quark (eq) final states, they may also be observed at the TeVatron. Indeed, LQ production with decay to eq is excluded in a large proportion of the phase space accessible at HERA by recent TeVatron measurements [6,7]. This does not apply for other LQ decays, so, in addition to the inclusive LQ search made by studying the lepton-quark mass ($\sqrt{xs}$) spectrum, an explicit search for events in which a LQ has decayed to μq or τq was performed. The signature of these events is the observation of an azimuthally separated quark jet and lepton (μ or τ, respectively). No such events were observed and this, together with the inclusive results, enables limits to be placed on the production of LQs as a function of their decay branching ratio to eq (β_e), to $e\mu$, to τq (β_τ), of the LQ coupling to positrons and quarks (λ_e) and of the LQ mass (M_{LQ}). For example, figure 1 shows the regions in the (M_{LQ}, λ_e) plane excluded by this study for various values of β_e and β_τ for LQs which couple to positrons and u quarks. Note the large area accessible to the HERA experiments which has not yet been covered at other colliders.

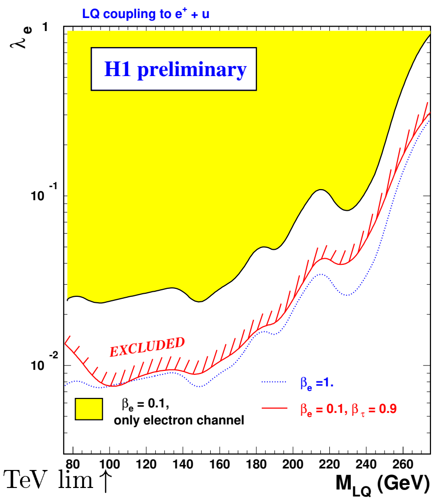

Figure 1: H1 limits on possible LQ masses and couplings for various decay branching ratios with current TeVatron limit for $\beta_e = 0.1$, $\beta_\tau = 0.9$.

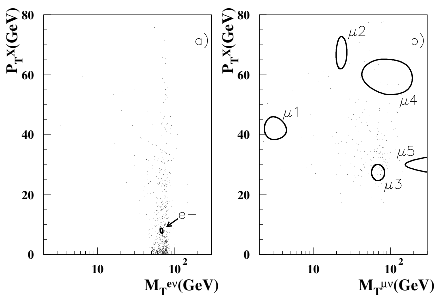

Figure 2: Distribution in (P_T^X, $M_T^{l\nu}$) plane of a) e events, b) μ events; error ellipses indicate data, dots the dominant SM contribution, from W production, for a luminosity 500 times that of the data.

2.4 Lepton events with missing hadronic p_T

H1 has observed a handful of events containing an isolated lepton and a quark jet with large momentum transverse to the beams. These are not compatible kinematically with being the result of LQ decays, but are of interest in their own right as the rate observed is higher than expected. One such event has been described in [8] and discussed further in [9].

A generalized search was performed for events with characteristics similar to the above, that is with large missing transverse momentum $\not{P}_T^{cal}$, measured using all calorimetric energy deposits, and containing isolated charged particles. Six such events were found. In 5 cases the isolated track was found to be a muon of which two had negative charge, two positive charge and one such high transverse momentum that the charge proved unmeasurable. The remaining event contained a negatively charged electron. All known SM sources of such events were considered, including: W production, $e^+q \to eq'W$; Z production; CC and NC DIS; photoproduction, particularly of heavy quarks, and two-photon interactions. The most likely source of these isolated lepton events is W production with the subsequent decay $W \to l\nu$. Leading order (LO) Monte Carlo calculations [10] show that, given the experimental selection criteria, one to two such events are expected with $l = e$ and less than one with $l = \mu$; all other processes together are expected to contribute less than one additional event to either channel.

The possibility that the isolated lepton events are the result of W production was further examined by studying the distribution of the events in the $(P_T^X, M_T^{l\nu})$ plane, where P_T^X is the magnitude of the transverse component of the total hadronic momentum, $\vec{P}_T^X$, and $M_T^{l\nu} = \sqrt{(\not{P}_T + P_T^l)^2 - (\vec{\not{P}}_T + \vec{P}_T^l)^2}$ is the transverse mass of the $l\nu$ system, assuming the missing momentum to result from the escaping ν in the W decay. The quantity P_T^l is the magnitude of the charged lepton's transverse momentum, $\vec{P}_T^l$. These distributions are shown separately for the electron and muon events in figure 2 as they are affected differently by the requirement that there be significant $\not{P}_T^{cal}$. The data are compared with the expectation from the above Monte Carlo for a luminosity a factor of 500 greater than that of the data. It is apparent that, while the electron and two of the muon events are in regions likely to be populated by W production, there are three muon events in a region in which W production is unlikely.

3 Inclusive cross section measurements

3.1 Introduction

The large increase in the amount of data available following the 1997 running has made possible the extension of NC and CC e^+p cross section measurements to higher Q^2 values and allowed the first double differential cross section measurements at high Q^2. Refinement of aspects of the experimental technique has allowed the NC cross section measurements to be pushed to very low x, with Q^2 still within the region in which perturbative QCD calculations are clearly applicable.

3.2 High Q^2 neutral current cross sections

New data, plus extensive work on the calibration of the H1 calorimeters, have allowed greatly extended measurements to be made of the cross section

$$\frac{d^2\sigma}{dx\,dQ^2} = \frac{2\pi\alpha^2}{xQ^4}\big(Y_+ F_2(x,Q^2) - y^2 F_L(x,Q^2) - Y_- xF_3(x,Q^2)\big),$$

where $Y_\pm = 1 \pm (1-y)^2$. The lower Q^2 cross sections presented to date [11] have been dominated by the electromagnetic part of the structure function F_2. At values of Q^2 around the Z^0 mass squared (M_Z^2), the effects of the parity violating structure function F_3 are appreciable. Results are presented here in the form of the reduced cross section

$$\sigma = \frac{xQ^4}{2\pi\alpha^2}\frac{1}{Y_+}\frac{d^2\sigma}{dx\,dQ^2}.$$

This, in double differential form, is shown in figure 3. The significance of electroweak effects increases as Q^2 rises above $10\,000\,\mathrm{GeV}^2$ as is most clearly seen in figure 4b). The effects of the larger than expected rate of events at the highest Q^2 values can be seen in figures 4c) and d).

The above results, presented in more detail in [12], illustrate the progress made at the high Q^2 frontier at HERA. Significant gains have also been made in the attempt to push measurements to the lowest possible values of x, while remaining in the perturbative regime. For a given centre-of-mass energy this requires that measurements be made at the largest possible values of y, *i.e.* scattered positrons of low energy must be detected. Progress in this respect is illustrated in figure 5, which includes measurements up to $y = 0.82$. Here, the contribution of the longitudinal structure function F_L becomes significant, and indeed this allows a measurement of F_L to be made [13]. Also shown in figure 5 is the QCD expectation which, intriguingly, at the lowest x values tends to lie above the data for $Q^2 \lesssim 20\,\mathrm{GeV}^2$. Further data will show whether this is the first indication of the effects of gluon recombination within the proton.

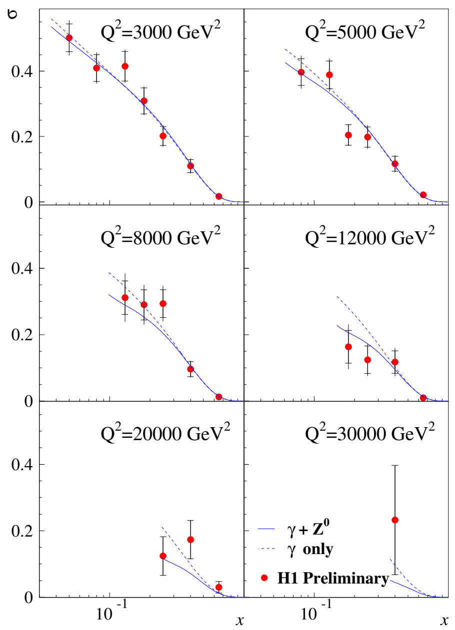

Figure 3: The e^+p NC DIS cross section presented as a function of x in various Q^2 regions. In this and all subsequent figures, the inner error bars indicate the statistical errors and the outer error bars the quadratic sum of the statistical and systematic uncertainties.

3.3 High Q^2 charged current cross sections

The SM charged current e^+p scattering cross section may be represented in terms of the quark and anti-quark parton distribution functions, $d(x,Q^2)$, $s(x,Q^2)$, $\bar{u}(x,Q^2)$ and $\bar{c}(x,Q^2)$ as follows:

$$\frac{d^2\sigma_{CC}}{dx\,dQ^2} = \frac{G_F^2}{2\pi}\left(\frac{M_W^2}{M_W^2+Q^2}\right)^2 \big(\bar{u}+\bar{c}+(1-y)^2(d+s)\big),$$

where M_W is the mass of the W boson. In analogy with the NC case, a reduced cross section is defined:

$$\sigma = \frac{2\pi x}{G_F^2}\left(\frac{Q^2+M_W^2}{M_W^2}\right)^2 \frac{d^2\sigma_{CC}}{dx\,dQ^2} = x\big(\bar{u}+\bar{c}+(1-y)^2(d+s)\big).$$

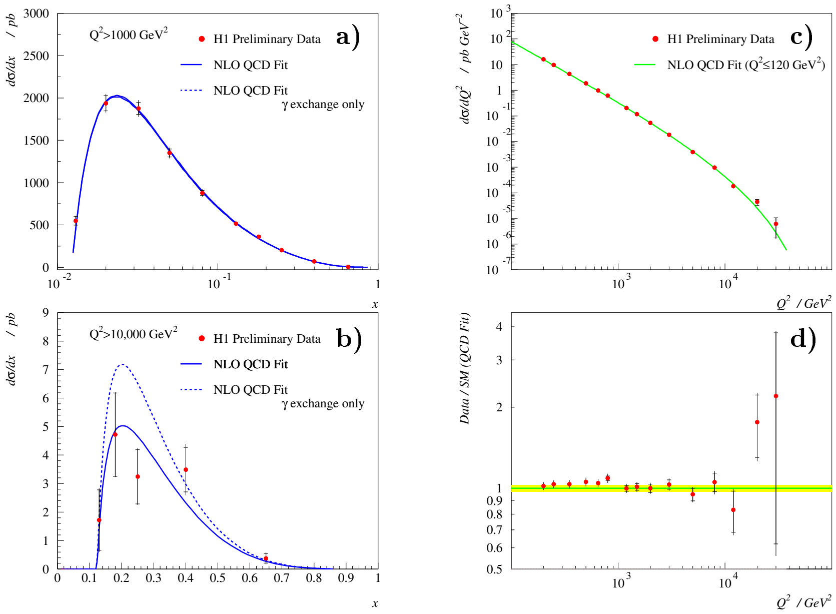

Figure 4: The e^+p NC DIS cross sections, a) and b) as a function of x in two ranges of Q^2, and c) as a function of Q^2; d) shows the ratio of the cross section as a function of Q^2 to the SM expectation. Indicated as a band in d) is the 2.6% uncertainty arising from the luminosity measurement.

The first ever double differential measurements of the CC cross section in the kinematic region made accessible by HERA are presented in figure 6. These measurements are shown as a function of Q^2 in figure 7a), integrated over the region $x > 0.01$ and $0.03 < y < 0.9$. The ratio of the measurements to SM expectation is presented in figure 7b); again at the highest Q^2 values it is apparent that the measurements lie above the expectation, although this discrepancy is in itself not statistically significant. In figure 7c) are shown the NC and CC cross sections as a function of Q^2 for all x and the region $y < 0.9$. At high Q^2, where the suppression of weak effects due to the W and Z masses is removed, the NC and CC cross sections are observed to be similar.

4 Description of the hadronic final state

4.1 Introduction

The above results show that, with the possible exception of the highest Q^2 values, the SM describes beautifully the H1 inclusive NC and CC DIS cross

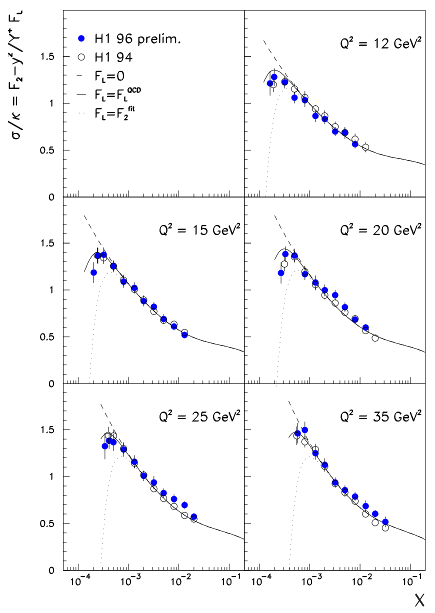

Figure 5: The reduced NC DIS e^+p cross section as a function of x in various Q^2 regions with the QCD expectation and the expectations allowed by the most extreme possible choices for F_L.

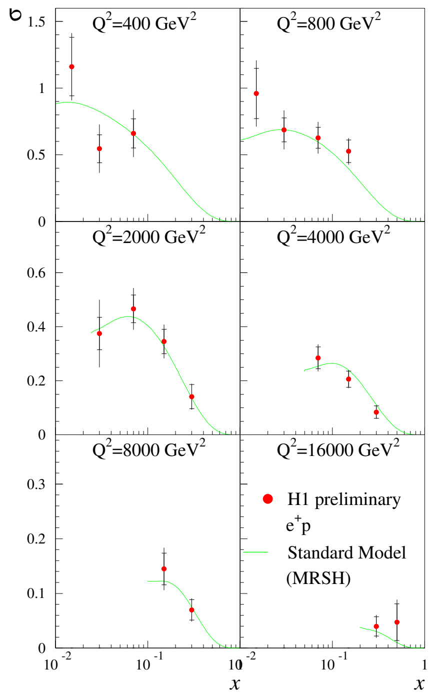

Figure 6: The CC DIS e^+p cross section presented as a function of x in various Q^2 regions.

section measurements. We now consider the more difficult task of understanding the hadronic final state. The discussion centres on the description of di-jet rates, where perturbative QCD is expected to be applicable, the search for clear signatures of BFKL-like evolution and the modelling of aspects of the final state for which hadronisation models are required.

4.2 Di-jet rates in DIS

The measurements of the di-jet rate presented at DIS97 were as much as a factor 2 larger than next-to-leading order (NLO) QCD predictions [15]. It has since been realised that the comparisons were being made in a region in which the NLO calculations are subject to large corrections [16]. The problem arises when both jets have similar transverse energies and can be circumvented by demanding, for example, that the lowest transverse energy jet have $E_{t,1} >$

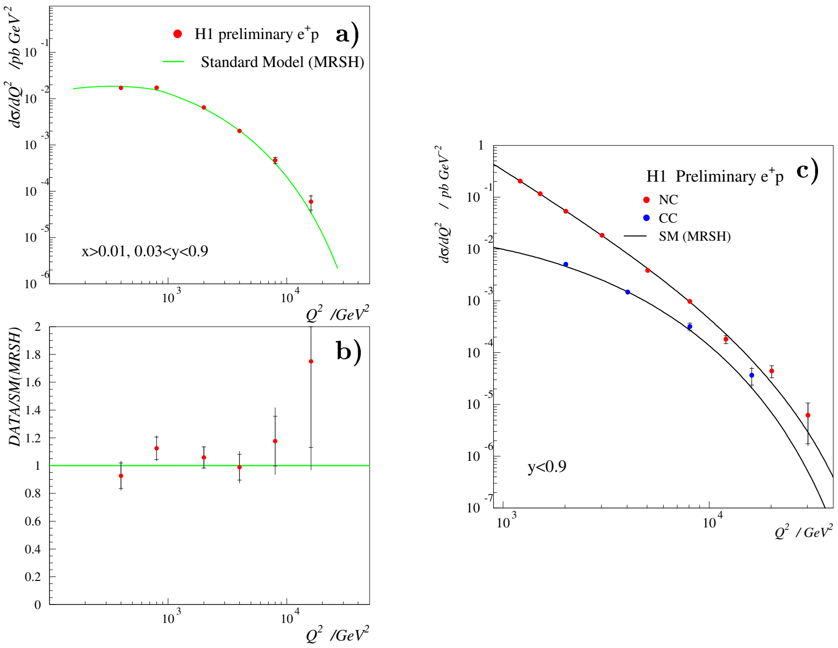

Figure 7: a) The CC DIS e^+p cross section as a function of Q^2, b) the ratio of the CC cross section as a function of Q^2 to the SM expectation, c) the NC and CC DIS e^+p cross sections. Not shown in b) is the 2.6% uncertainty arising from the luminosity measurement.

5 GeV and that the sum of the jet transverse energies satisfy $\sum_{i=1,2} E_{t,i} >$ 17 GeV. NLO calculations then give a good description of the data at high Q^2, as shown in figure 8, in which the longitudinally invariant k_t algorithm [17] was used in the Breit frame to define the jets [18]. This figure also illustrates the importance of the choice of renormalization scale. Whereas setting $\mu_r^2 = Q^2$ allows a good description of the data over the entire Q^2 range, the choice $\mu_r^2 = Q^2 + E_t^2$ results in a prediction that undershoots the data at low Q^2. The latter choice seems preferable, however, as it would appear to allow the description of the region in which $E_t^2 \gg Q^2$. An intuitively appealing picture which explains the failure of the NLO calculations with $\mu_r^2 = Q^2 + E_t^2$ in this region, is that they do not include a contribution for the eventuality that the structure of the virtual photon, size $\sim 1/Q$, is resolved by the probing parton from the proton, wavelength $\sim 1/E_t$. The effect of including this resolved photon contribution is shown in figure 9, in which the jets are defined using a cone algorithm [19] applied in the hadronic centre-of-mass frame. The deficit at low Q^2 is successsfully

accounted for. Such measurements may also be used to extract information on the partonic structure of the virtual photon, as described in [20]. Figure 9 also illustrates the lack of sensitivity to the precise mechanism used to ensure that the data are not dominated by jets with similar energies; figures 9a) and b) used the requirement $E_{t,1} > 5\,\mathrm{GeV}$ and $E_{t,2} > 7\,\mathrm{GeV}$, whereas in figures 9c) and d) it was required that $E_{t,1} > 5\,\mathrm{GeV}$ and that $\sum_{i=1,2} E_{t,i} > 13\,\mathrm{GeV}$.

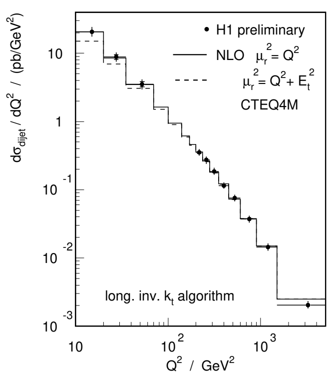

Figure 8: Di-jet cross section over full Q^2 range compared with NLO QCD calculations using differing renormalization scales.

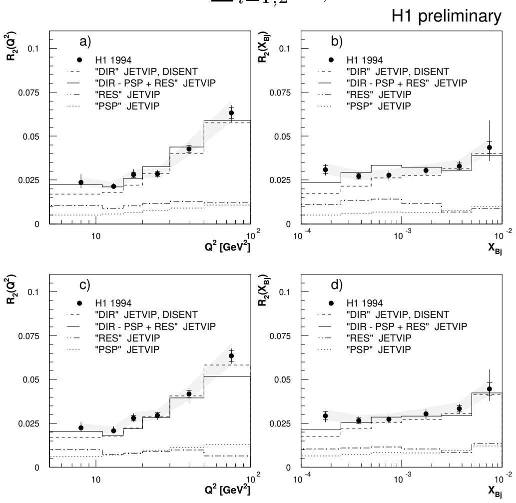

Figure 9: Di-jet cross sections in DIS as a function of a) Q^2 and b) x, showing the direct ("DIR") and resolved ("RES") photon contributions. The sum of these ("DIR - PSP + RES"), avoiding double counting of the photon splitting part of the cross section ("PSP"), accurately describes the data; c) and d) are as a) and b) but with differing jet selection criteria - see text.

4.3 Forward π studies

A continuing discussion at HERA concerns the regions of validity of the QCD evolution schemes used in structure function calculations, such as those of BFKL [21] and DGLAP [22]. It has been established that inclusive measurements, *e.g.* $F_2(x, Q^2)$, are not sensitive to the differences in these schemes [23]. However, some evidence has been found for the necessity of including BFKL or BFKL-like evolution in studies of the hadronic final state; in particular the transverse momentum spectrum of hadrons travelling in the proton remnant or forward direction in low x DIS events is harder than expected in DGLAP based models [24], the forward jet cross section [25] and the rate of production of high energy forward π^0 mesons in DIS [26] are somewhat higher than DGLAP predictions and the transverse momentum spectrum of diffractively produced J/ψ mesons is harder than expected in models without a BFKL inspired contribution [28]. The π^0 measurement has now been extended to the study of forward charged particles. The results, shown in figure 10 and described in [27], support the necessity for producing more high momentum partons in the forward direction than can be accommodated in unadulterated DGLAP calculations.

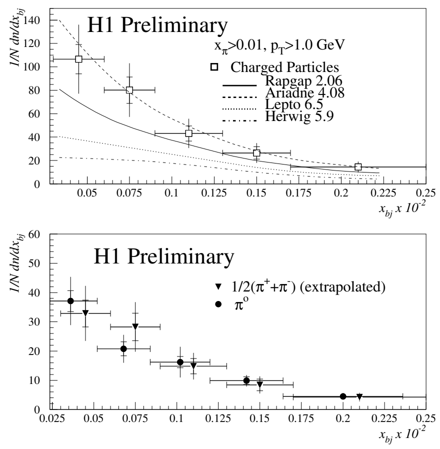

Figure 10: Top, cross section for charged particle production in the region $x_\pi = E_\pi/E_p > 0.01$ as a function of x compared with various MC predictions. Bottom, cross section for $\pi^\pm$ production compared with π^0 measurements in the same kinematic region.

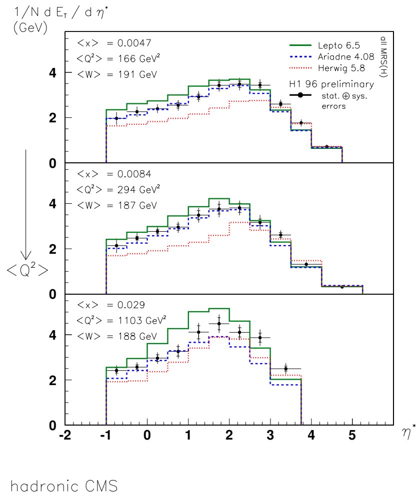

Figure 11: The E_T flow in the hadronic centre-of-mass as a function of pseudorapidity in various Q^2 intervals compared with a selection of Monte Carlo models.

4.4 E_T flow at high Q^2

Shown in figure 11 are measurements of the energy flow transverse to the $\gamma^* p$ axis in the hadronic centre-of-mass frame presented as a function of pseudorapidity ($\eta^\star$) in various regions of Q^2. The evolution with Q^2 of these results, cannot be described by any of the QCD inspired Monte Carlo models shown, as is discussed in [29].

5 Event shape studies

5.1 Introduction

The above demonstrates that NLO QCD calculations provide a good description of di-jet production in DIS, which enables the measurement of α_S in DIS [30,31] and the study of its running. In principle, similar measurements can be made via studies of infra-red safe event shape variables such as thrust or jet broadening, generically labelled F here. The accuracy of these has been limited by the necessity of modelling the hadronisation process, which is poorly understood, as demonstrated by the E_T results above. Recently, new ideas on power suppressed corrections to QCD observables like the F have been developed [32] and applied to DIS [33]. These allow the description of the form and magnitude of the effects up to an approximately universal parameter $\bar{\alpha}_0(\mu_I^2)$ which can be considered to be related to the strength of the coupling below the scale μ_I^2 at which the perturbative description of the F fails.

5.2 Evolution of event shapes with Q

The above motivates a fit to the data on the evolution of event shape variables with Q using the form

$$\langle F \rangle = \langle F^{pert} \rangle + \langle F^{power} \rangle,$$

where F^{pert} represents the NLO QCD expectation, dependent on α_S, and F^{power} is the "power correction" term, proportional to $1/Q$ for the F considered here and containing the parameter $\bar{\alpha}_0(\mu_I^2)$. This ansatz allows the accurate description of the evolution with Q of many event shape variables [34], as is illustrated in figure 12 in which the F are measured in the current hemisphere of the Breit frame. The value of $\bar{\alpha}_0(\mu_I^2)$ extracted from the fits to the evolution of the various F is consistently around 0.5, lending some support to the idea that a universal description of the effects below the perturbative regime is possible.

5.3 Description of event shape distributions

The possibility of extending the above idea to the description of the distributions of the F has recently been discussed [35]. Here it is examined if an ansatz of the form

$$\frac{d\sigma}{dF} = \frac{d\sigma^{pert}(F - \langle F^{power} \rangle)}{dF}$$

can describe the data. Figure 13 shows that this appears to be the case for a limited range of the shape variables F. Measurements of event shapes and

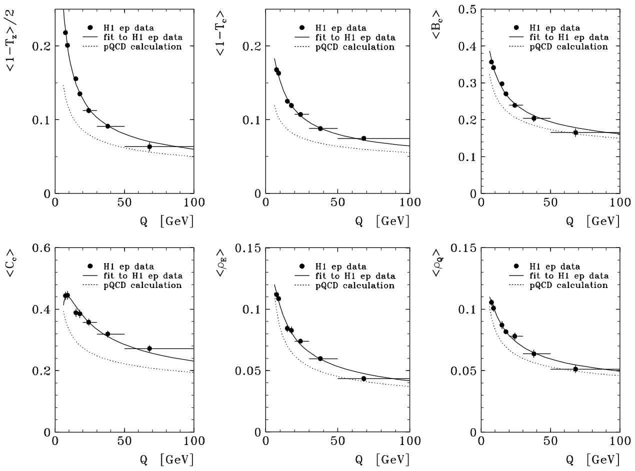

Figure 12: Evolution with Q of the mean values of various event shape variables measured in the Breit Frame compared with NLO QCD expectations and with fits based on the "power correction" ansatz.

their evolution with Q are discussed in detail in [36]. Study of higher order terms in the power corrections in DIS (see [37]) will hopefully allow these methods to provide competitive measurements of α_S and improve our understanding of some non-perturbative aspects of QCD.

6 Heavy flavour

6.1 Introduction

Heavy quarks are produced in DIS at HERA predominantly via boson gluon fusion [38]. They "remember" the momentum of the gluon from which they originate, and hence can be used to extract the contribution the gluon makes to proton structure. Heavy quarks are also produced in the interactions of real photons with the proton, so similar studies are also possible in photoproduction; both approaches are discussed in [39]. Here, the former technique is presented, as is the first HERA measurement of the open beauty photoproduction cross section.

6.2 Extraction of the gluon density from charm in DIS

The presence of open charm in the final state of DIS events was tagged by the observation of $D^{\star\pm}$ mesons, detected via the decay chain $D^{\star+} \rightarrow D^0\pi^+ \rightarrow (K^-\pi^+)\pi^+$ and its charge conjugate. To LO, the fractional gluon momentum

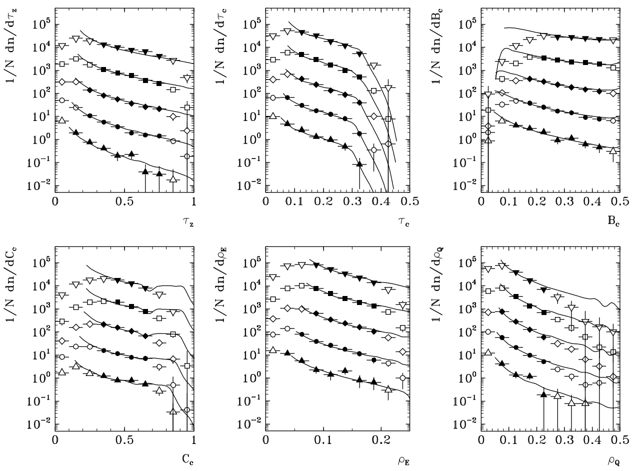

Figure 13: Breit frame measurements of various event shape distributions compared with the NLO QCD expectations and a fit using the "power correction" ansatz.

is given by $x_g = \frac{\hat{s}+Q^2}{ys}$, where $\hat{s}$ is the squared $\gamma g \to c\bar{c}$ sub-process centre-of-mass energy. Experimentally, $x_g^{obs} \sim x_g$ was determined by replacing $\hat{s}$ above with $\hat{s}_{obs}$, where

$$\hat{s}_{obs} = \frac{(1.2p_T^\star)^2 + m_c^2}{z(1-z)},\ z = \frac{(E-p_z)_{D^\star}^{lab}}{2yE_e},$$

$p_T^\star$ is the momentum of the $D^\star$ transverse to the virtual photon proton axis in the hadronic centre-of-mass frame and E_e is the positron beam energy. From the measurement of x_g^{obs}, the gluon density in the proton was unfolded using the NLO calculations described in [40]. The result is shown in figure 14, compared with the gluon density extracted from the study of the scaling violations of F_2 [41,42]. The agreement of these two results and of the gluon density extracted from photoproduction measurements demonstrates the consistency of the different aspects of QCD used in the analysis.

6.3 Measurement of the open beauty photoproduction cross section

The open beauty cross section was measured in photoproduction ($Q^2 < 1\,\mathrm{GeV}^2$ and $0.1 < y < 0.8$) using the semi-muonic decay of the b to tag beauty events. As is described in [43], the selection required that events contain at least two jets with $E_T > 6\,\mathrm{GeV}$ and at least one muon in the range $35° < \theta_\mu < 130°$ with $p_T^\mu > 2\,\mathrm{GeV}$. The spectrum of the momentum of the muons transverse to the

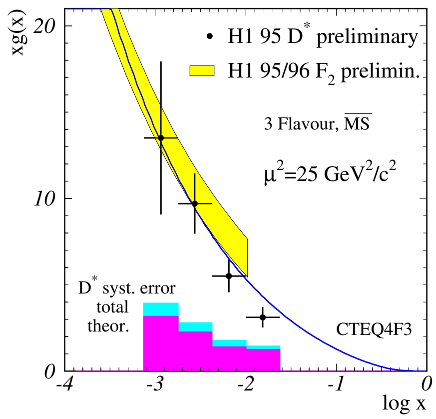

Figure 14: The gluon distribution in the proton from measurements of charm in DIS (points) compared with the distribution extracted from the analysis of the scaling violations of F_2.

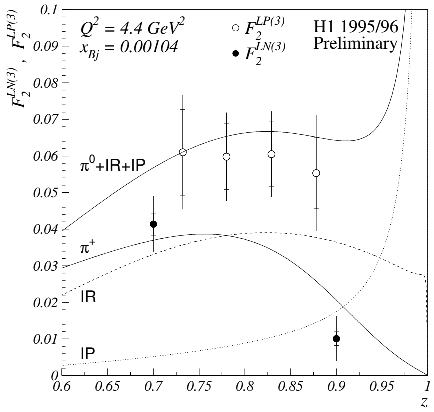

Figure 15: The structure functions $F_2^{LP(3)}$ and $F_2^{LN(3)}$ in the region $z > 0.6$ compared to a Regge model of baryon production which includes pion, $I\!P$ and $I\!R$ exchanges. The n data are described by π^+ exchange, the p data by the sum of $I\!P$, $I\!R$ and π^0 exchanges, the latter (not shown) is exactly half that of the π^+ contribution.

jets with which they were associated ($p^{\mu}_{T,rel}$) was measured and the background contribution to this extracted from the data using a detailed parameterization of the muon mis-identification probability, obtained from studies of K^0, ϕ and Λ decays. Comparison of the $p^{\mu}_{T,rel}$ spectrum with the shapes expected for the b and c contributions from the AROMA Monte Carlo[44] allowed the determination of the cross-section in the above kinematical range. The result,

$$\sigma_{vis}(ep \to b\bar{b}X) = 0.93 \pm 0.08^{+0.21}_{-0.12}\,\mathrm{nb},$$

is a factor of five larger than the LO expectation, obtained from the above Monte Carlo.

7 Rapidity gap events

7.1 Introduction

H1 have demonstrated that DIS events with the structure $ep \to eXY$, where the systems X and Y are separated by the largest rapidity gap in the event,

Y has small mass and the squared four-momentum transfer between the incoming proton and Y is small, can be described in terms of a Regge based model involving a Pomeron ($I\!P$) trajectory and a sub-leading Reggeon exchange ($I\!R$) [45,46], provided Y carries a large proportion, $z \gtrsim 0.95$, of the proton's momentum. This picture is also borne out by studies of the hadronic final state in such events [47,48]. The possibility that other models are able to describe the data is considered in [49]. Here, we concentrate on the extension of the above studies to the cases in which Y is a nucleon (N), *i.e.* either a p measured in the Leading Proton Spectrometer, or a n, measured in the Forward Neutron Calorimeter [50], and concentrate on the range $0.6 \lesssim z \lesssim 0.9$. In this region the Regge model predicts that an important contribution to the cross section will result from π^0 exchange in the p case and that π^+ exchange will dominate in the case of the n.

7.2 Leading baryon measurements

The measurements are presented in terms of the leading baryon structure functions $F_2^{LB(3)}$, defined through the expression

$$\frac{d^3\sigma(ep \to eNX)}{dx\, dQ^2\, dz} = \frac{4\pi\alpha^2}{xQ^4}\Big(1 - y + \frac{y^2}{2[1 + R(x, Q^2, z)]}\Big) F_2^{LB(3)}(x, Q^2, z),$$

where R is the ratio of the longitudinal to the transverse photon absorption cross sections; $R \sim 0$ here. An integration over the transverse momentum of the outgoing baryon has been performed in the range $0 < p_T < 200\,\mathrm{MeV}$. Figure 15 shows the measurements of these structure functions together with the expectations of model calculations based on the $I\!P$, $I\!R$ and π^0 exchange ansatz for the leading proton case ($F_2^{LP(3)}$) and π^+ exchange for the leading neutron case ($F_2^{LN(3)}$) which are found to give a good description of the data. These measurements allow constraints to be placed on the structure of the pion.

8 Summary

A brief discussion was presented of some areas of ep scattering in which the last year has seen a particularly marked advance in our knowledge. These include studies of the highest Q^2 neutral current (NC) and charged current (CC) e^+p DIS events, searches for new physics, double differential measurements of the high Q^2 NC and CC e^+p cross sections, searches for leptoquarks, jet studies, energy flow results, searches for the effects of BFKL-like evolution in the hadronic final state, event shape studies, the extraction of the gluon density using

DIS events containing charm, the measurement of the open beauty photoproduction cross section and studies of leading baryon production. In many of these areas the Standard Model (SM) performs well and future efforts must be directed towards improving the precision of the measurements. In others there are discrepancies suggesting that our understanding is incomplete: there is (still) an excess of events at the highest values of Q^2; more events containing high transverse momentum (p_T) leptons with large missing hadronic p_T are observed than expected; despite much effort, the modelling of many features of the hadronic final state is poor, and the open beauty photoproduction cross section is a factor of 5 larger than expected. Finally, there are areas where recent work will hopefully allow us to connect more closely the fundamental theories of the SM with measurements made in ep scattering. Event shape studies look particularly promising in this respect, and progress is being made in the study of rapidity gap phenomena.

Acknowledgments

I would like to thank all those who so competently organised this exciting workshop, and all the members of the H1 Collaboration whose hard work and thought made possible the advances discussed above. Particular thanks are due to Jörg Gayler and Martin Erdmann for the careful reading of this manuscript.

References

1. C. Adloff *et al.* (H1 Collaboration), Zeit. Phys. **C74** (1997) 191.
2. J. Breitweg *et al.* (ZEUS Collaboration), Zeit. Phys. **C74** (1997) 207.
3. Proc. of workshop "Future Physics at HERA", Hamburg 1996, ed.s G. Ingelman, A. DeRoeck and R. Klanner, Vol. 2, page 1133.
4. S. Aid *et al.* (H1 Collaboration), Phys.Lett. **B369** (1996) 173.
5. M.C. Cousinou, these proceedings.
6. F. Abe *et al.* (CDF Collaboration), Phys. Rev. Lett. **79** (1997) 4327;
   B. Abbott, *et al.* (D0 Collaboration), Phys. Rev. Lett. **80** (1998) 2051;
   B. Abbott, *et al.* (D0 Collaboration), Phys. Rev. Lett. **79** (1997) 4321;
   S. Abachi, *et al.* (D0 Collaboration), Phys. Rev. Lett. **75** (1995) 3618.
7. I. Bertram, these proceedings;
   L. Demortier, these proceedings.
8. T. Ahmed *et al.* (H1 Collaboration), DESY preprint, DESY 94-248 (1994).
9. T. Ahmed *et al.* (H1 Collaboration), Zeit. Phys. **C71** (1996) 211.
10. U. Baur, J.A.M Vermaseren, D. Zeppenfeld, Nucl. Phys. **B375** (1992) 3.

11. S. Aid *et al.* (H1 Collaboration), Phys. Lett. **B379** (1996) 319;
S. Aid *et al.* (H1 Collaboration), Zeit. Phys. **C67** (1995) 565.
12. B. Heinemann, these proceedings.
13. C. Adloff *et al.* (H1 Collaboration), Phys. Lett. **B393** (1997) 452.
14. S. Aid *et al.* (H1 Collaboration), Zeit. Phys. **C67** (1995) 565.
15. M. Wobisch, Proc. of the Int. Workshop on DIS and QCD, Chicago 1997.
16. S. Frixione and G. Ridolfi, Nucl. Phys. **B507** (1997) 315.
17. S.D. Ellis and D.E. Soper, Phys. Rev. **D48** (1993) 3160;
S. Catani, Yu.L. Dokshitzer, M.H. Seymour and B.R. Webber, Nucl. Phys. **B406** (1993) 187.
18. M. Wobisch, these proceedings.
19. M.H. Seymour, Zeit. Phys. **C62** (1994) 545.
20. M. Taševský, these proceedings.
21. E.A. Kuraev, L.N. Lipatov and V.S. Fadin, Sov. Phys. JETP **45** (1977) 199;
Ya.Ya. Balitsky and L.N. Lipatov, Sov. J. Nucl. Phys. **28** (1978) 822;
J. Bartels and H. Lotter, Phys. Lett. **B309** (1993) 400.
22. V.N. Gribov and L.N. Lipatov, Sov. J. Nucl. Phys. **15** (1972) 438;
G. Altarelli and G. Parisi, Nucl. Phys. **B126** (1977) 298;
Yu.L. Dokshitzer, Sov. Phys. JETP **46** (1977) 641.
23. A.J. Askew, J. Kwiecinski, A.D. Martin and P.J. Sutton, Phys. Lett. **B325** (1994) 21;
M. Glück, E. Reya and A. Vogt, Zeit. Phys. **C67** (1995) 433.
24. C. Adloff *et al.* (H1 Collaboration), Nucl. Phys. **B485** (1997) 3.
25. S. Aid *et al.* (H1 Collaboration), Phys. Lett. **B356** (1995) 118.
26. "Forward π^0 production at HERA", H1 Collaboration, to appear in Proc of the Int. Europhys. Conf. on HEP, Aug. 1997, Jerusalem, Israel.
27. T. Wengler, these proceedings.
28. P. Thompson, these proceedings.
29. D. Kruecker, these proceedings.
30. T. Ahmed *et al.* (H1 Collaboration), Phys. Lett. **B346** (1995) 415.
31. N. Tobien, these proceedings.
32. B.R. Webber, Phys. Lett. **B339** (1994) 148;
Yu.L. Dokshitzer and B.R. Webber, Phys. Lett. **B352** (1995) 451;
Yu.L. Dokshitzer, G. Marchesini and B.R. Webber, Nucl. Phys. **B469** (1996) 93;
P. Nason and M.H. Seymour, Nucl. Phys. **B454** (1995) 291;
R. Akhoury and V.I. Zakharov, Phys. Lett. **B357** (1995) 646 and Nucl. Phys. **B465** (1996) 295.
33. M. Dasgupta and B.R. Webber, Eur. Phys. Jour. **C1** (1998) 539.

34. C. Adloff *et al.* (H1 Collaboration), Phys. Lett. **B406** (1997) 256.
35. Yu.L. Dokshitzer and B.R. Webber, Phys. Lett. **B404** (1997) 321.
36. H.-U. Martyn, these proceedings.
37. Yu.L. Dokshitzer, A. Lucenti, G. Marchesini and G.P. Salam, hep-ph/9802381.
38. C. Adloff *et al.* (H1 Collaboration), Nucl. Phys. **B472** (1996) 32.
39. D. Müller, these proceedings.
40. B.W. Harris and J. Smith, Nucl. Phys. **B452** (1995) 109.
41. S. Aid *et al.* (H1 Collaboration), Nucl. Phys. **B470** 3.
42. E. Rizvi, these proceedings
43. G. Tsipolitis, these proceedings.
44. G. Ingelman, J. Rathsman and G.A. Schuler, DESY preprint, DESY 96-058 (1996), and hep-ph/9605285.
45. T. Ahmed *et al.* (H1 Collaboration), Phys. Lett. **B348** (1995) 681;
C. Adloff *et al.* (H1 Collaboration), Zeit. Phys. **C76** (1997) 613.
46. T. Nicholls, these proceedings.
47. C. Adloff *et al.* (H1 Collaboration), Eur. Phys. Jour. **C1** (1998) 495;
C. Adloff *et al.* (H1 Collaboration), DESY preprint, DESY-98-029 (1998) and hep-ex/9803032;
C. Adloff *et al.* (H1 Collaboration), DESY preprint, DESY-98-044 (1998) and hep-ex/9804012.
48. B. Waugh, these proceedings.
49. M. Wüsthoff, these proceedings.
50. T. Nunnemann, these proceedings.